Supporting information

Composition-driven Shape Evolution to Cu-rich PtCu Octahedral Alloy Nanocrystals as Superior Bifunctional Catalysts for Methanol Oxidation and Oxygen Reduction Reaction

Chaozhong Li,[a,b] Taiyang Liu,[a] Ting He,[b] Bing Ni,[b] Qiang Yuan,*[a,b] Xun Wang*[b]

[a]Department of Chemistry, College of Chemistry and Chemical Engineering, Guizhou University, Guiyang, Guizhou province 550025, P. R. China.
E-mail: qyuan@gzu.edu.cn
[b]Department of Chemistry, Tsinghua University, Beijing 100084, P. R. China.
E-mail: wangxun@mail.tsinghua.edu.cn

Experimental section:

Chemicals: Platinum(II) acetylacetonate ($Pt(acac)_2$, 97%), copper(II) acetylacetonate ($Cu(acac)_2$, 97%) were purchased from Sigma-Aldrich. Hexadecyl trimethyl ammonium Bromide (CTAB，99%), Glucose (99%), N,N-Dimethylformamide (DMF, 99.8%) were purchased from Aladdin. Formaldehyde (99.5%) were purchased from Alfa Aesar. Pt black and Pt/C (20 wt%) catalyst was purchased from Johnson Matthey. Chemicals were used as received without further purification. The super pure water (18.25MΩ cm) was used as solvent for electrochemical test.

Synthesis of octahedral $Pt_{34.5}Cu_{65.5}$ nanoparticles

In a typical synthesis octahedral $Pt_{34.5}Cu_{65.5}$ nanoparticles: 12 mg of $Pt(acac)_2$, 15.8 mg of $Cu(acac)_2$, 90.1 mg of Glucose and 36.4 mg of Hexadecyl trimethyl ammonium Bromide (CTAB) were added into 7 mL DMF solution and 1 ml Formaldehyde solution under magnetic stirring. The resulting homogeneous mixture was transferred to a 10 mL Teflon-lined stainless-steel autoclave. The sealed vessel was then heated at 180°C for 12 hours before it was cooled to room temperature. The products were separated three times by centrifugation and washing cycles at 10,000 rpm for 15 minutes with ethanol. The collected product was redispersed in ethanol.

Synthesis of Pt cubes

In a typical synthesis Pt cubes: 12 mg of $Pt(acac)_2$, 90.1 mg of Glucose and 36.4 mg of Hexadecyl trimethyl ammonium Bromide (CTAB) were added into 7 mL DMF solution and 1 ml Formaldehyde solution under magnetic stirring. The resulting homogeneous mixture was transferred to a 10 mL Teflon-lined stainless-steel autoclave. The sealed vessel was then heated at 180°C for 12 hours before it was cooled to room temperature. The products were separated three times by centrifugation and washing cycles at 10,000 rpm for 15 minutes with ethanol. The collected product was redispersed in ethanol.

Characterizations: The size and morphology of the nanocrystals were determined by a HITACHI H-7700 transmission electron microscope (TEM) at 100 kV, and a FEI

Tecnai G2 F20 S-Twin high- resolution transmission electron microscope (HRTEM) equipped with energy dispersive spectrometer (EDS) analyses at 200 kV. The high-angle annular dark-field scanning TEM (HAADF-STEM) was determined by a FEI Tecnai G2 F20 S-Twin HRTEM operating at 200 kV. The X-ray diffraction (XRD) patterns of the samples were recorded on a Bruker D8 Advance diffractometer with Cu Kα radiation (λ=1.5418 Å) with graphite monochromator (40 KV, 40 mA). X-ray photoelectron spectroscopy (XPS) measurements were performed using a PHI Quantum 2000 Scanning ESCA Microprobe (Physical Electronics, USA), using Al K_α X-ray radiation (1486.6 eV) for excitation. Binding energies were corrected from charge effects by reference to the C1s peak of carbon at 284.8 eV. The inductively coupled plasma optical emission spectrometry (ICP-OES) analysis of samples was performed on IRIS Intrepid II XSP (ThermoFisher).

Characterization of electrocatalytic activity:

Electrochemical experiments were carried out in a standard three-electrode cell at room temperature controlled by CHI 760E electrochemical analyzer (CHI Instruments, Shanghai, Chenghua Co., Ltd.). The super pure water (18.25 MΩ cm) purified through a Milli-Q Lab system (Nihon Millipore Ltd.) was used as solvent. The working electrode is a glassy carbon (GC, Φ=5 mm) electrode embedded into a Teflon holder. Prior to the electrochemical test, the GC electrode was mechanically polished using successively alumina powder of size 1.5, 0.5, and 0.05 μm. It was then cleaned in an ultrasonic bath. Then took a certain amount of $Pt_{34.5}Cu_{65.5}$ and Pt black catalyst powder and dispersed with super pure water under ultrasonic bath. The suspension of nanocrystals was spread on the GC electrode. As soon as the electrode was dried under infrared lamp, 4 μL Nafion diluents (1 wt.% Nafion® solution) was coated onto the electrode surface. A Ag/AgCl electrode and a platinum foil were used as the reference and counter electrode, respectively. The cyclic voltammograms (CVs) were obtained in nitrogen-saturated 0.1M H_2SO_4 solution, and the potential was scanned from□0.25 to 0.9 V (Ag/AgCl) at a scan rate 50 mV s^{-1}. The scan was repeated several times to ensure that a stable cyclic voltammetry (CV) was obtained.

Voltammogram measurements for methanol oxidation were carried out in 0.1 M H_2SO_4+0.5 M methanol solution, and the potential was scanned from -0.25 to 0.9 V (Ag/AgCl) at a scan rate 50 mV s^{-1}. Electrochemical CO stripping on $Pt_{34.5}Cu_{65.5}$ and Pt black was tested in 0.1 M H_2SO_4 saturated with CO at scan rate of 50 mV s^{-1}.

Electrochemical experiments of ORR were performed using a glassy carbon rotating disk electrode (RDE) (PINE, USA). The ORR measurements were conducted at room temperature in 0.1 M H_2SO_4 solutions after a flow of O_2 an half hour until saturated, then using a glassy carbon rotating disk electrode (RDE) at a rotation rate of 1600 rpm, and the potential was scanned from 0.1 to 1.1 V (vs. RHE) at a scan rate of 10 mV s^{-1}. The kinetic current (i_k) can be derived from the experimental data using the well-known Koutecky-Levich equation: ($1/i = 1/i_k + 1/i_L$) at 0.90 V, where i_L and i are the diffusion limiting current and measured current (0.90V) at kinetic-diffusion control region, respectively.

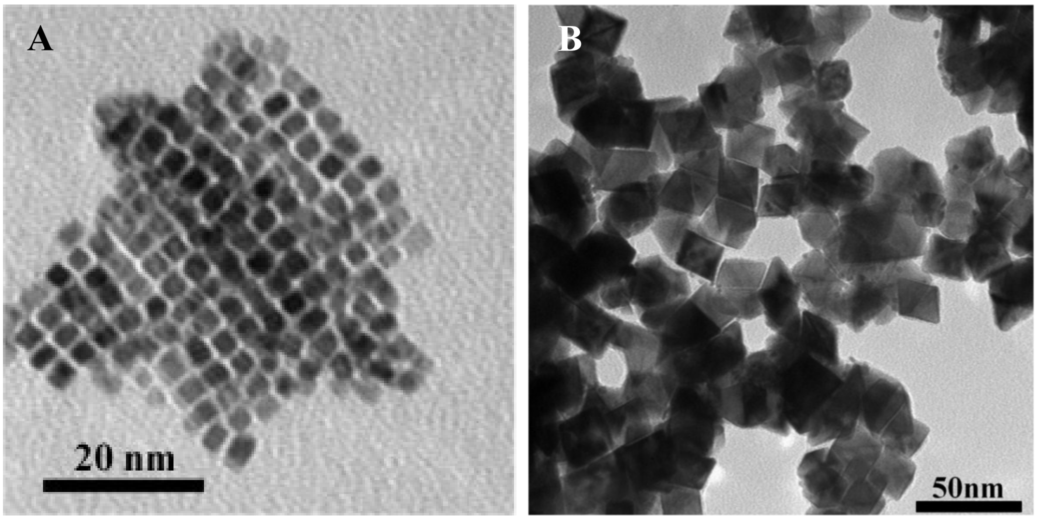

Fig. S1 TEM images of the as-synthesized Pt cubes (A) and $Pt_{34.5}Cu_{65.5}$ octahedrons (B).

Sample	**Element**	**Atom feeding ratio**	**Atom% (result of ICP)**
$Pt_{73.3}Cu_{26.7}$	Pt Cu	3 1	73.3 26.7
$Pt_{63.9}Cu_{36.1}$	Pt Cu	2 1	63.9 36.1
$Pt_{52.0}Cu_{48.0}$	Pt Cu	1 1	52.0 48.0
$Pt_{34.5}Cu_{65.5}$	Pt Cu	1 2	34.5 65.5

Table S1. The composition of the as-synthesized PtCu products calculated from ICP-OES.

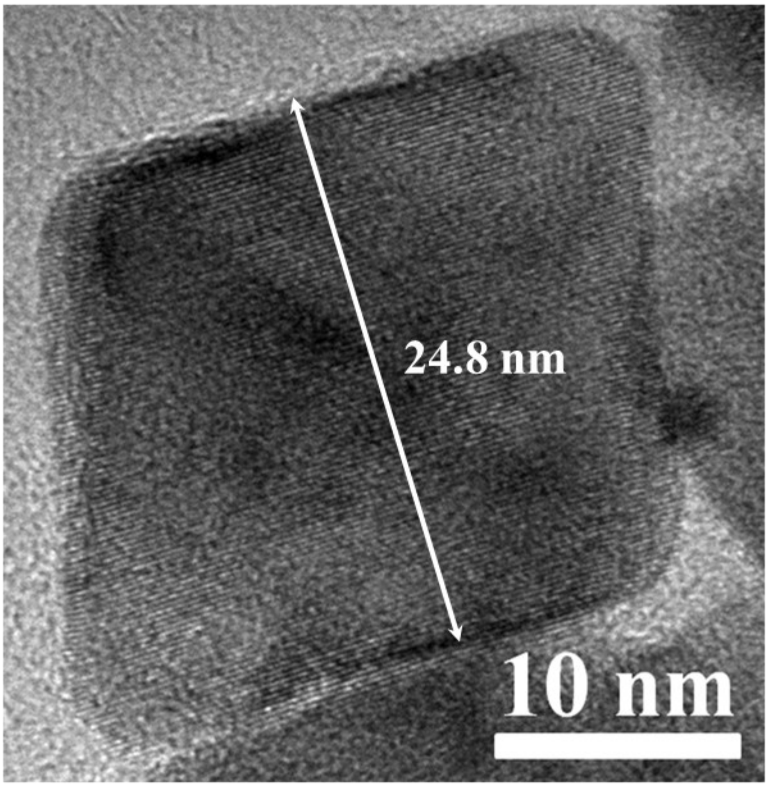

Fig. S2 HRTEM images of the as-synthesized $Pt_{34.5}Cu_{65.5}$ octahedrons.

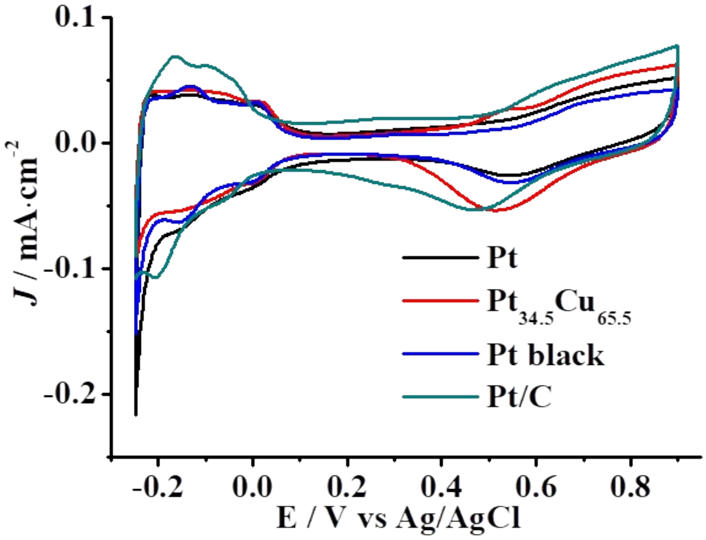

Fig. S3 The cyclic voltammetric curves (CVs) of the as-synthesized Pt Cubes, $Pt_{34.5}Cu_{65.5}$ octahedrons, commercial Pt black and Pt/C in 0.1M H_2SO_4 solution.

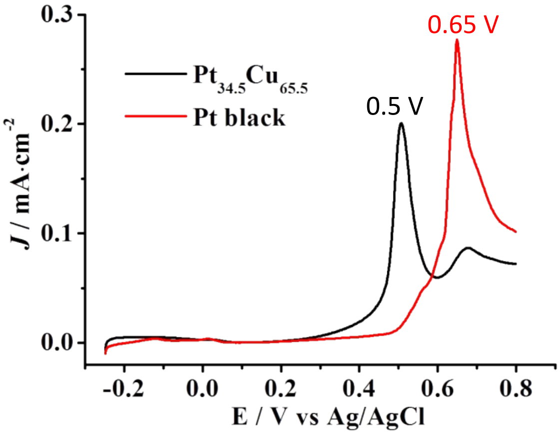

Fig. S4 LSV curves of electrochemical CO stripping on $Pt_{34.5}Cu_{65.5}$ octahedrons and commercial Pt black in 0.1 M H_2SO_4 saturated with CO at scan rate of 50 mV s^{-1}.

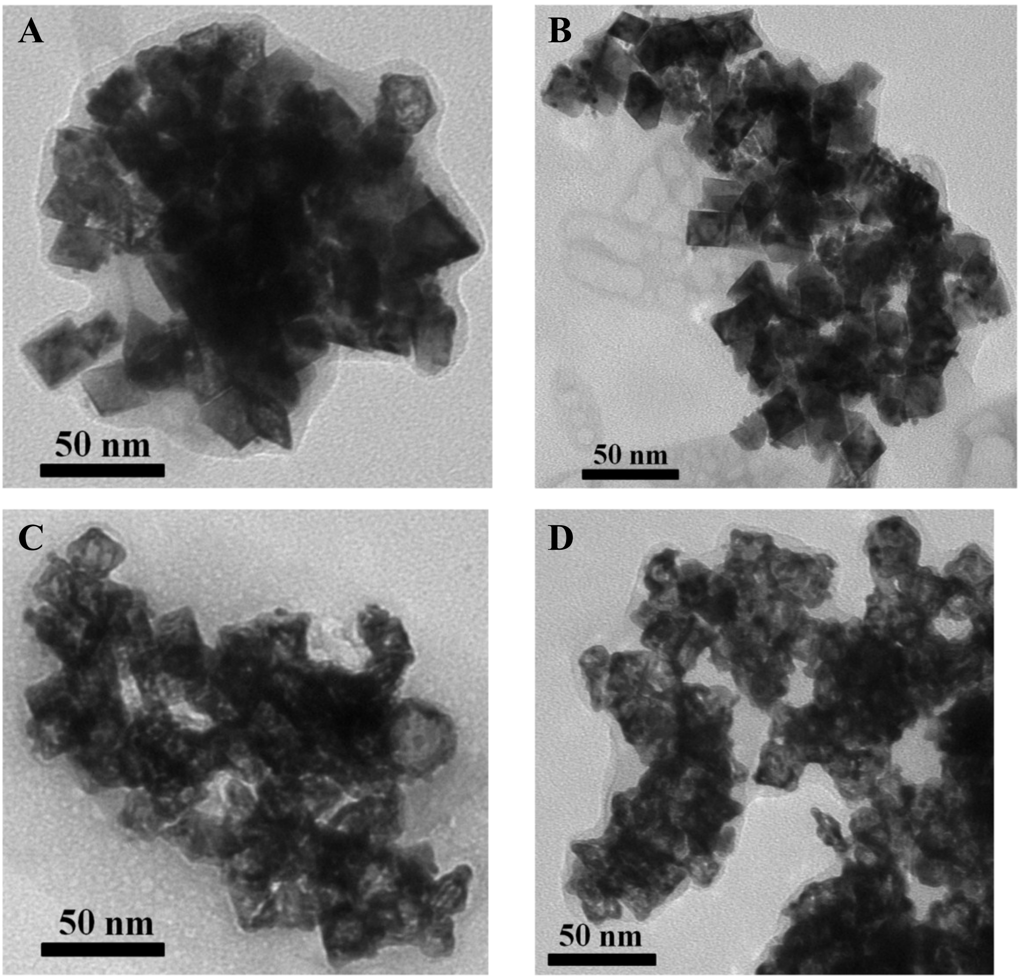

Fig. S5 The TEM images of $Pt_{34.5}Cu_{65.5}$ octahedrons after current-time test (A, B) and ORR after 5000 cycles of ADTs test (C, D).

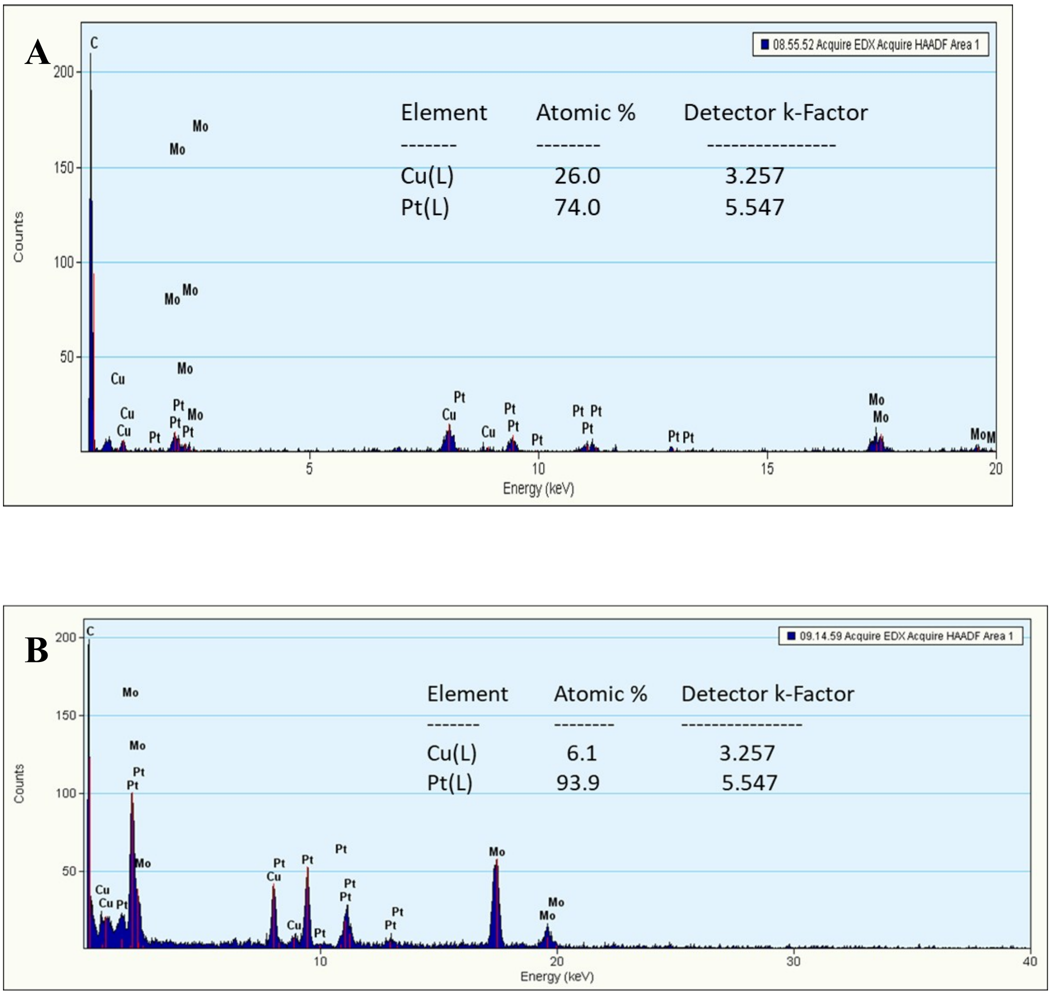

Element	Atomic %	Detector k-Factor
Cu(L)	26.0	3.257
Pt(L)	74.0	5.547

Element	Atomic %	Detector k-Factor
Cu(L)	6.1	3.257
Pt(L)	93.9	5.547

Fig. S6 The EDS spectra of $Pt_{34.5}Cu_{65.5}$ octahedrons after current-time test (A) and 5000 cycles accelerated durability test (B). (The signals of MO came from Mo grids.)

Catalysts	**Test conditions**	**Specific Activities ($mA\cdot cm^{-2}$)**	**Mass Activities ($A\cdot mg^{-1}_{Pt}$)**	**References**
Star-like PtCu/rGO	0.5 M H_2SO_4 + 1 M CH_3OH; Scan rate: 50 mV· s^{-1}	NA	0.67	27
Dendritic Pt_3Cu Triangular Pyramid Caps	0.5 M H_2SO_4 + 1 M CH_3OH; Scan rate:50 mV· s^{-1}	0.73	0.5	28
PtCu alloy yolk–shell cubes	0.5 M H_2SO_4 + 0.5 M CH_3OH; Scan rate: 20 mV· s^{-1}	0.78	NA	29
$PtCu_2$ NWNs	0.5 M H_2SO_4 + 1 M CH_3OH; Scan rate:50 mV· s^{-1}	1.87	1.287	30
Branched Pt-Cu	NA	1.26	0.698	31
Pt-Cu BANDs	0.5 M H_2SO_4 + 1 M CH_3OH; Scan rate:50 mV· s^{-1}	1.51	0.355	32
Pt−Cu yolk-cage alloy	0.5 M H_2SO_4 + 2 M CH_3OH; Scan rate:50 mV· s^{-1}	2.8	NA	33
Pt_3Cu nanodendrites	0.1 M $HClO_4$ + 1 M CH_3OH; Scan rate:50 mV· s^{-1}	0.50	NA	34
Screw Thread-Like PtCu Nanowires	0.1 M $HClO_4$ + 0.2 M CH_3OH; Scan rate:50 mV· s^{-1}	3.31	1.56	35
Pt-Ni-Cu ROH	0.5 M H_2SO_4 + 2 M CH_3OH; Scan rate:50 mV· s^{-1}	2.61	0.065	36
$Pt_{34.5}Cu_{65.5}$ octahedrons	0.1 M H_2SO_4 + 0.5 M CH_3OH; Scan rate:50 mV· s^{-1}	4.12	1.43	This work

Table S2. Summary of literature catalytic parameters of various PtCu-based MOR catalysts.

References:

27. Chen D, Zhao Y, Peng X, et al. Star-like PtCu nanoparticles supported on graphene with superior activity for methanol electro-oxidation. *Electrochimica Acta*, **2015**, 177:86-92.

28. Kuang Y, Cai Z, Zhang Y, et al. Ultrathin dendritic Pt_3Cu triangular pyramid caps with enhanced electrocatalytic activity. *ACS Applied Materials & Interfaces*, **2014**, 6(20):17748.

29. Ye S H, He X J, Ding L X, et al. Cu_2O template synthesis of high-performance PtCu alloy yolk-shell cube catalysts for direct methanol fuel cells. *Chemical Communications*, **2014**, 50(82):12337-40.

30. Xiao M, Li S, Zhao X, et al. Enhanced Catalytic Performance of Composition-Tunable PtCu Nanowire Networks for Methanol Electrooxidation. *Chemcatchem*, **2015**, 6(10):2825-2831.

31. Cao Y, Yang Y, Shan Y, et al. One-Pot and Facile Fabrication of Hierarchical Branched Pt-Cu Nanoparticles as Excellent Electrocatalysts for Direct Methanol Fuel Cells. *ACS Applied Materials & Interfaces*, **2016**, 8(9):5998-6003.

32. Gong M, Fu G, Chen Y, et al. Autocatalysis and selective oxidative etching induced synthesis of platinum-copper bimetallic alloy nanodendrites electrocatalysts. *ACS Applied Materials & Interfaces*, **2014**, 6(10):7301.

33. Zhang Z, Yang Y, Nosheen F, et al. Fine tuning of the structure of Pt-Cu alloy nanocrystals by glycine-mediated sequential reduction kinetics. *Small*, **2014**, 9(18):3063-3069.

34. Taylor E, Chen S, Tao J, et al. Synthesis of Pt-Cu nanodendrites through controlled reduction kinetics for enhanced methanol electro-oxidation. *Chemsuschem*, **2013**, 6(10):1863-1867.

35. Zhang N, Bu L, Guo S, et al. Screw Thread-Like Platinum-Copper Nanowires Bounded with High-Index Facets for Efficient Electrocatalysis. *Nano Letters*, **2016**, 16(8):5037.

36. Pengfang Zhang, Xiaoping Dai, Xin Zhang, et al. One-Pot Synthesis of Ternary Pt–Ni–Cu Nanocrystals with High Catalytic Performance. *Chemistry of Materials*, **2015**, 27(18):6402-6410.

Catalysts	**Test conditions**	**Specific Activities ($mA\cdot cm^{-2}$)**	**Mass Activities ($A\cdot mg^{-1}_{Pt}$)**	**References**
$Pt_{78}Cu_{22}$ BANDs	0.1M $HClO_4$; scan rate:20 $mV\cdot s^{-1}$	0.63	0.32	37
PtCu-250	0.1M $HClO_4$; scan rate:20 $mV\cdot s^{-1}$	2.30	1.06	38
PdCu@PtCu/C	0.1M $HClO_4$; scan rate:50 mV·s-1	0.9764	0.4002	39
PtCu NWs	0.1M $HClO_4$; scan rate:10 $mV\cdot s^{-1}$	0.404	0.216	40
PtNiCu multi-rods/C	0.1M $HClO_4$; scan rate:10 $mV\cdot s^{-1}$	0.26	0.063	41
$Pt_{34.5}Cu_{65.5}$ octahedrons	0.1M H_2SO_4; scan rate:10 $mV\cdot s^{-1}$	1.70	0.59	This work

Table S3. Summary of literature catalytic parameters of various PtCu-based ORR catalysts.

References:

37. Fu S, Zhu C, Shi Q, et al. Highly branched PtCu bimetallic alloy nanodendrites with superior electrocatalytic activities for oxygen reduction reactions. *Nanoscale*, **2016**, 8(9):5076-5081.
38. Wittkopf J A, Zheng J, Yan Y. High-Performance Dealloyed PtCu/CuNW Oxygen Reduction Reaction Catalyst for Proton Exchange Membrane Fuel Cells. *ACS Catalysis*, **2014**, 4(9):3145-3151.
39. Li Y, Chen L, Chen K, et al. Monodisperse PdCu@PtCu Core@Shell nanocrystal and their high activity and durability for oxygen reduction reaction. *Electrochimica Acta*, **2016**, 192:227-233.
40. Chen B, Cheng D, Zhu J. Synthesis of PtCu nanowires in nonaqueous solvent with enhanced activity and stability for oxygen reduction reaction. *Journal of Power Sources*, **2014**, 267(3):380-387.
41. Liu L, Samjeské G, Takao S, et al. Fabrication of PtCu and PtNiCu multi-nanorods with enhanced catalytic oxygen reduction activities. *Journal of Power Sources*, **2014**, 253(5):1-8.